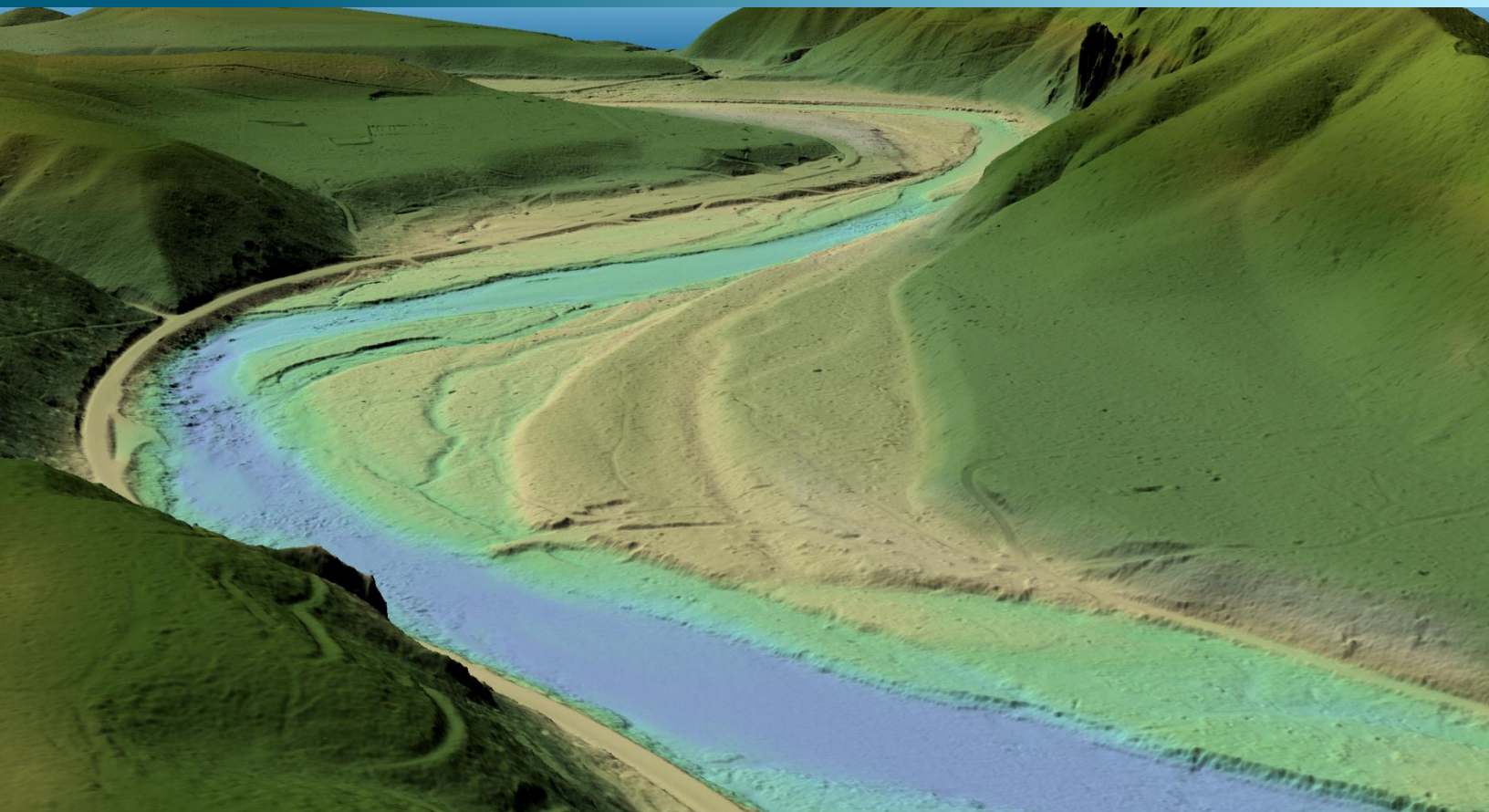


January 21, 2022



McKenzie River Corridor, Oregon Topobathymetric Lidar Technical Data Report

Task Order: 140G00221F0198
Project ID: 221670

Contract: G16PC00016
Work Unit ID: 221667

Prepared For:



United States Geological Survey
1400 Independence Road
Rolla, MO 65401

Prepared By:



NV5 Geospatial Corvallis
1100 NE Circle Blvd, Ste. 126
Corvallis, OR 97330
PH: 541-752-1204

TABLE OF CONTENTS

INTRODUCTION	1
Deliverable Products	2
ACQUISITION	4
Planning.....	4
Turbidity Measurements and Secchi Depth Readings.....	4
Airborne Survey.....	9
Lidar	9
Digital Imagery.....	13
Ground Survey.....	14
Base Stations.....	14
Ground Survey Points (GSPs).....	15
Land Cover Class	16
USGS Survey Collaboration.....	18
PROCESSING	20
Topobathymetric Lidar Data	20
Bathymetric Refraction	23
Lidar Derived Products	23
Topobathymetric DEMs.....	23
Digital Imagery	24
RESULTS & DISCUSSION.....	25
Bathymetric Lidar	25
Mapped Bathymetry and Depth Penetration.....	25
Lidar Point Density	26
First Return Point Density.....	26
Bathymetric and Ground Classified Point Densities	26
Lidar Accuracy Assessments.....	30
Lidar Non-Vegetated Vertical Accuracy.....	30
Lidar Bathymetric Vertical Accuracies	33
Lidar Vegetated Vertical Accuracies	35
Lidar Relative Vertical Accuracy	36
Lidar Horizontal Accuracy	37
Digital Imagery Accuracy Assessment.....	37
CERTIFICATIONS	38
GLOSSARY	39
APPENDIX A – ACCURACY CONTROLS.....	40
APPENDIX B – USGS SURVEY SUMMARY	41

Cover Photo: A view looking East over the McKenzie River near Eagle Rock. The image was created from the lidar bare earth model colored by elevation.

INTRODUCTION

This photo taken by NV5 Geospatial acquisition staff shows a view of ground survey equipment set up for collection of ground check points within the McKenzie River Corridor topobathy project area in Oregon.



In July 2021, NV5 Geospatial (NV5) was contracted by the United States Geologic Survey (USGS) to collect topobathymetric Light Detection and Ranging (lidar) data and digital imagery in the summer of 2021 for the McKenzie River Corridor site in Oregon. The McKenzie River Corridor area of interest includes a tight boundary around approximately 13 square miles of the McKenzie river, starting up river near the West Trail Bridge Dam and following the river's flow east into Eugene, ending near Hileman Landing. Traditional near-infrared (NIR) lidar was fully integrated with green wavelength return data (bathymetric) lidar in order to provide a seamless topobathymetric lidar dataset. Data was collected to aid the USGS Oregon Water Science Center's fish habitat restoration project, U.S. Army Corp of Engineer's evaluation of the impact of recent wildfires on the McKenzie River basin's hydrology, and the USGS 3DEP mission.

This report accompanies the delivered topobathymetric lidar data and imagery, and documents contract specifications, data acquisition procedures, processing methods, and analysis of the final dataset including lidar accuracy, and density. Acquisition dates and acreage are shown in Table 1, a complete list of contracted deliverables provided to USGS is shown in Table 2, and the project extent is shown in Figure 1.

Table 1: Acquisition dates, acreage, and data types collected on the McKenzie River Corridor site

Project Site	Contracted Acres	Acquisition Dates	Data Type
McKenzie River Corridor, Oregon	8,216	07/26/2021- 07/28/2021	Topobathymetric Lidar
			3 band (RGB) Digital Imagery

Deliverable Products

Table 2: Products delivered to USGS for the McKenzie River Corridor site

McKenzie River Corridor Lidar Products Projection: Oregon Statewide Lambert Horizontal Datum: NAD83 (2011) Vertical Datum: NAVD88 (GEOID18) Units: International Feet	
Topobathymetric Lidar	
Points	LAS v 1.4 <ul style="list-style-type: none"> All Classified Returns
Rasters	2.0 Foot Cloud Optimized GeoTiffs (*.tif) <ul style="list-style-type: none"> Topobathymetric Bare Earth Digital Elevation Model (DEM) - tiled <ul style="list-style-type: none"> Clipped Unclipped Highest Hit Digital Surface Model (DSM) - tiled Swath Separation Images - tiled
Vectors	Shapefiles (*.shp) <ul style="list-style-type: none"> Area of Interest Lidar and Raster Tile Index Orthoimagery Tile Index ESRI File Geodatabase (*.gdb) <ul style="list-style-type: none"> Ground Survey Points Lidar Flightline Index Photo Flight Index Flightline Swath Coverage Extents Bathymetric Coverage Shape Water's Edge Breaklines Bridge Breaklines
3 Band (RGB) Digital Imagery	
Digital Imagery	6 inch GeoTiffs <ul style="list-style-type: none"> Tiled Imagery Mosaics (RGB) 6 inch MrSID Compression <ul style="list-style-type: none"> AOI Imagery Mosaic (RGB)

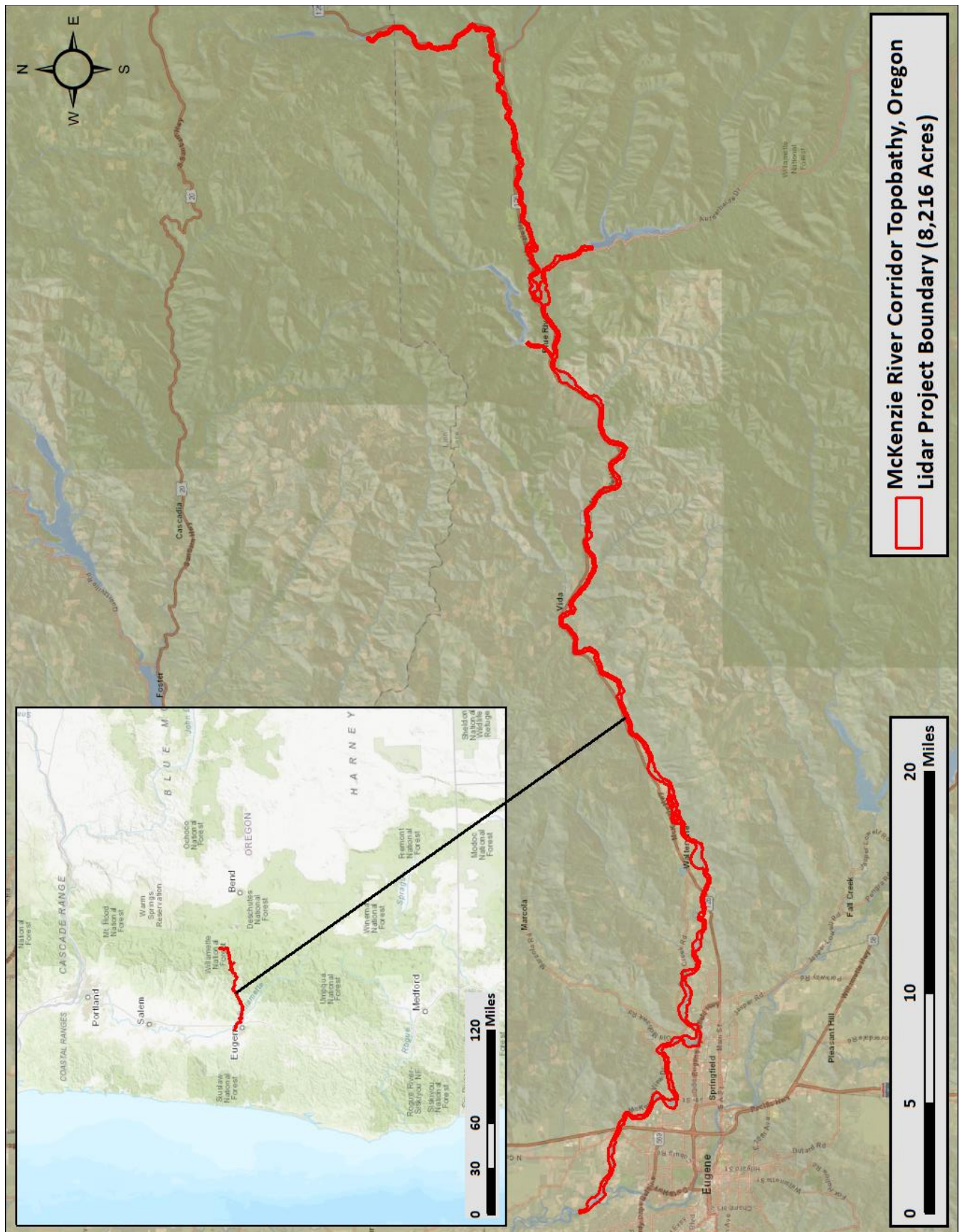


Figure 1: Location map of the McKenzie River Corridor site in Oregon

NV5's Cessna Caravan.



Planning

In preparation for data collection, NV5 reviewed the project area and developed a specialized flight plan to ensure complete coverage of the McKenzie River Corridor Lidar study area at the target combined point density of ≥ 8 points/m². Acquisition parameters including orientation relative to terrain, flight altitude, pulse rate, scan angle, and ground speed were adapted to optimize flight paths and flight times while meeting all contract specifications.

Factors such as satellite constellation availability and weather windows must be considered during the planning stage. Any weather hazards or conditions affecting the flight were continuously monitored due to their potential impact on the daily success of airborne and ground operations. In addition, logistical considerations including private property access, potential air space restrictions, channel flow rates (Figure 2 through Figure 5), and water clarity were reviewed.

Turbidity Measurements and Secchi Depth Readings

In order to assess water clarity conditions prior to and during lidar and digital imagery collection, NV5 collected turbidity measurements at seven locations and secchi depth readings at ten locations within the project site. Turbidity observations were recorded three to four times to confirm measurements. The tables below (Table 3 and Table 4) provide turbidity and secchi depth results per site. Please note that some secchi depth readings were noted to have reached the bottom surface of the riverbed.

Table 3: Secchi Observations for Lidar flights

Secchi Depth Observations			
Location	Longitude	Latitude	*Secchi Depth (m)
SECCHI_01	122°51'17.84"W	44° 3'35.29"N	3.00*
SECCHI_02	122°53'53.21"W	44° 3'37.38"N	3.05*
SECCHI_03	122°57'50.23"W	44° 4'17.16"N	5.10*
SECCHI_04	123° 2'44.33"W	44° 6'43.36"N	2.80*
SECCHI_05	122°36'51.67"W	44° 7'33.59"N	3.60*
SECCHI_06	122°38'23.09"W	44° 6'39.95"N	5.95
SECCHI_07	122°43'15.43"W	44° 5'26.95"N	3.30*
SECCHI_08	122°46'7.62"W	44° 4'10.86"N	4.45*
SECCHI_09	122°48'53.79"W	44° 3'16.36"N	4.60*
SECCHI_10	122°22'49.53"W	44° 7'41.72"N	3.60*

** Measurement is depth to the bottom surface due to observational depth limitations*

Table 4: Turbidity Observations for Lidar flights

Turbidity Depth Observations							
Location	Longitude	Latitude	Turbidity Read 1 (NTU)	Turbidity Read 2 (NTU)	Turbidity Read 3 (NTU)	Turbidity Read 4 (NTU)	Average Turbidity (NTU)
TURB_01	122°51'16.66"W	44° 3'34.62"N	0.03	0.00	0.00	N/A	0.01
TURB_02	122°57'52.25"W	44° 4'19.87"N	0.00	0.00	0.34	0.00	0.09
TURB_03	123° 2'53.26"W	44° 6'44.43"N	0.00	0.01	0.05	N/A	0.02
TURB_04	122°36'52.89"W	44° 7'33.50"N	0.14	0.00	0.00	N/A	0.05
TURB_05	122°46'7.76"W	44° 4'11.84"N	0.12	0.00	0.00	N/A	0.04
TURB_06	122°15'37.25"W	44° 9'49.58"N	0.05	0.00	0.00	N/A	0.02
TURB_07	122°22'49.73"W	44° 7'41.67"N	0.19	0.61	0.00	0.39	0.30

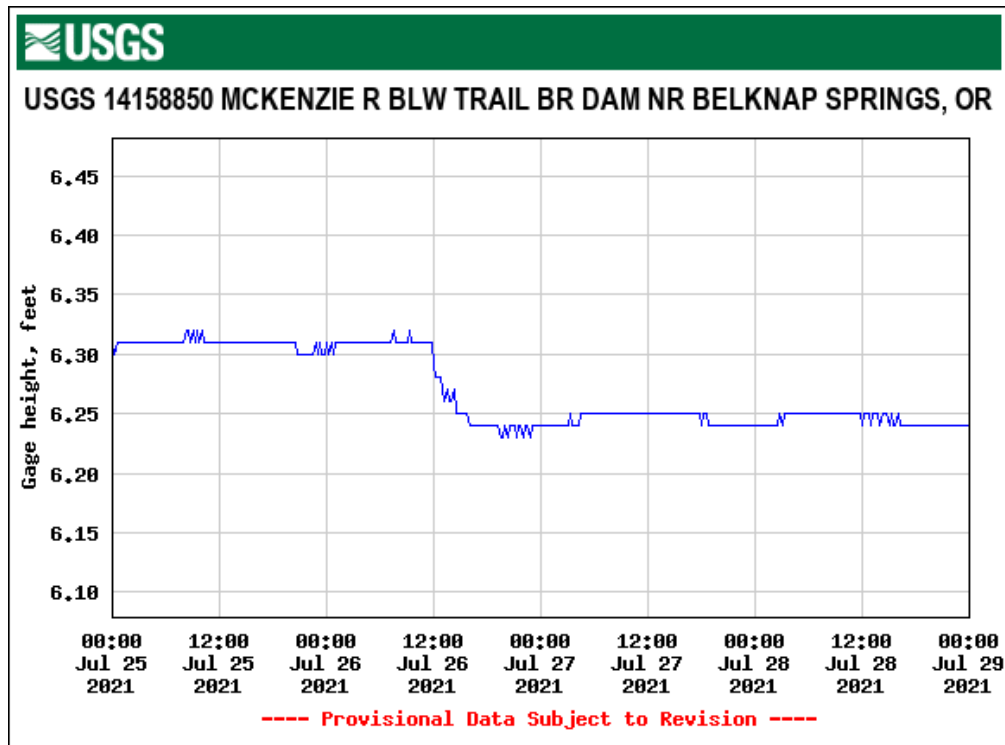


Figure 2: USGS Station 14158850 gage height nearest the top of the McKenzie River Corridor study site at the time of lidar acquisition.

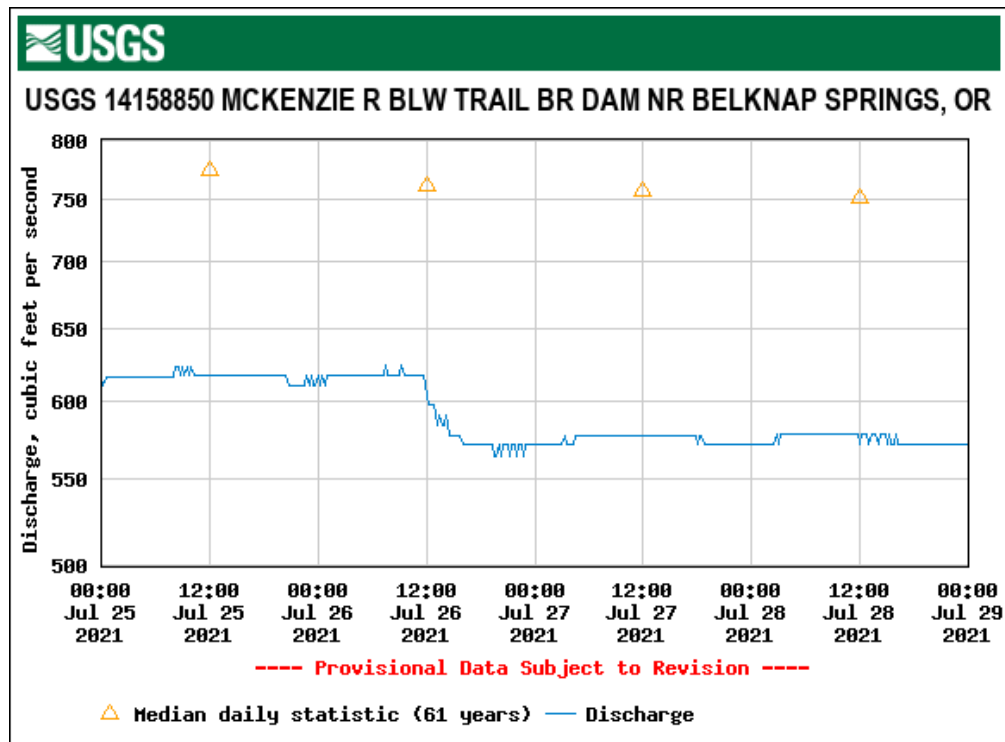


Figure 3: USGS Station 14158850 flow rates nearest the top of the McKenzie River Corridor study site at the time of lidar acquisition.

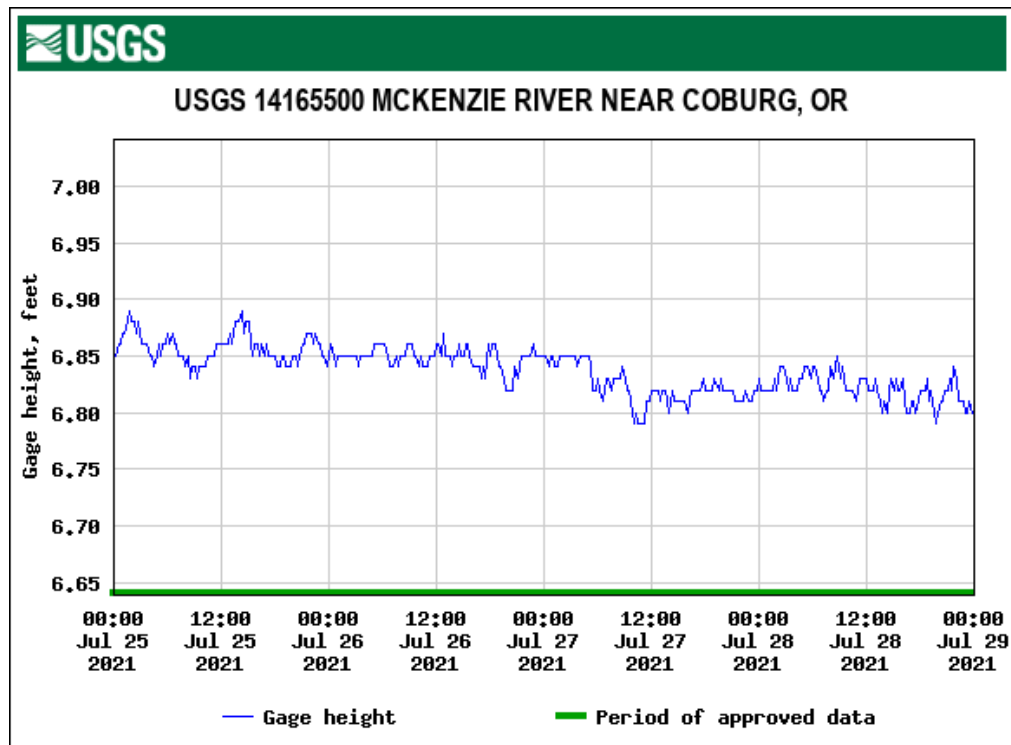


Figure 4: USGS Station 14165500 gage height nearest the bottom of the McKenzie River Corridor study site at the time of lidar acquisition.

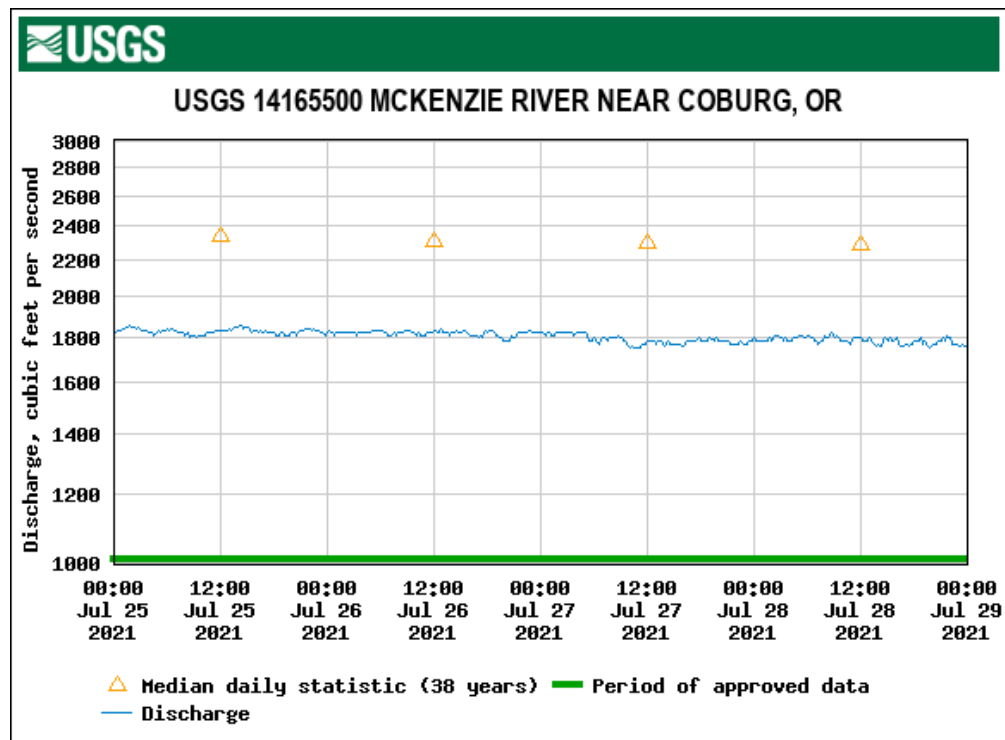


Figure 5: USGS Station 14165500 flow rates nearest the bottom of the McKenzie River Corridor study site at the time of lidar acquisition.



These photos taken by NV5 acquisition staff display water clarity conditions at two locations within the McKenzie River Corridor site.

Airborne Survey

Lidar

The lidar survey was accomplished using a Riegl VQ-880-GII green laser system mounted in a Cessna Caravan. The Riegl VQ-880-GII boasts a higher repetition pulse rate (up to 550 kHz), higher scanning speed, small laser footprint, and wide field of view which allows for seamless collection of high resolution data of both topographic and bathymetric surfaces. The green wavelength ($\lambda=532$ nm) laser is capable of collecting high resolution topography data, as well as penetrating the water surface with minimal spectral absorption by water. The Riegl VQ-880-GII contains an integrated NIR laser ($\lambda=1064$ nm) that adds additional topography data and aids in water surface modeling. The recorded waveform enables range measurements for all discernible targets for a given pulse. The typical number of returns digitized from a single pulse range from 1 to 14 for the McKenzie River Corridor project area. It is not uncommon for some types of surfaces (e.g., dense vegetation or water) to return fewer pulses to the lidar sensor than the laser originally emitted. The discrepancy between first return and overall delivered density will vary depending on terrain, land cover, and the prevalence of water bodies. All discernible laser returns were processed for the output dataset. Table 5 summarizes the settings used to yield an average pulse density of ≥ 8 pulses/m² over the McKenzie River Corridor project area.

Table 5: Lidar specifications and survey settings

Lidar Survey Settings & Specifications				
Acquisition Dates	July 26 - 28, 2021			
Aircraft Used	Cessna Caravan			
Sensor	Riegl			
Laser	VQ-880-GII - Green	VQ-880-GII - Green	VQ-880-GII - NIR	VQ-880-GII - NIR
Maximum Returns	Unlimited, but typically not more than 15	Unlimited, but typically not more than 15	Unlimited, but typically no more than 15	Unlimited, but typically not more than 15
Resolution/Density	Average 8 pulses/m ²	Average 8 pulses/m ²	Average 8 pulses/m ²	Average 8 pulses/m ²
Nominal Pulse Spacing	0.35 m	0.35 m	0.35 m	0.35 m
Survey Altitude (AGL)	400 m	600 m	400 m	600 m
Survey speed	140 knots	140 knots	140 knots	140 knots
Field of View	40°	40°	42°	42°
Mirror Scan Rate	80 lines per second	80 lines per second	uniform point spacing	uniform point spacing
Target Pulse Rate	200 kHz	200 kHz	150 kHz	150 kHz
Pulse Length	1.5 ns	1.5 ns	3 ns	3 ns
Laser Pulse Footprint Diameter	28 cm	42 cm	8 cm	12 cm
Central Wavelength	532 nm	532 nm	1064 nm	1064 nm
Pulse Mode	MTA (multiple times around)	MTA (multiple times around)	MTA (multiple times around)	MTA (multiple times around)
Beam Divergence	0.7 mrad	0.7 mrad	0.2 mrad	0.2 mrad
Swath Width	291 m	437 m	307 m	461 m
Swath Overlap	60%	60%	60%	60%
Intensity	16-bit	16-bit	16-bit	16-bit
Accuracy	RMSEz (Non-Vegetated) ≤ 10 cm	RMSEz (Non-Vegetated) ≤ 10 cm	RMSEz (Non-Vegetated) ≤ 10 cm	RMSEz (Non-Vegetated) ≤ 10 cm
	95% Confidence Level (Non-Vegetated) ≤ 19.6 cm	95% Confidence Level (Non-Vegetated) ≤ 19.6 cm	95% Confidence Level (Non-Vegetated) ≤ 19.6 cm	95% Confidence Level (Non-Vegetated) ≤ 19.6 cm
	Vegetated (95 th Percentile) ≤ 30 cm	Vegetated (95 th Percentile) ≤ 30 cm	Vegetated (95 th Percentile) ≤ 30 cm	Vegetated (95 th Percentile) ≤ 30 cm
	RMSEz (Bathymetric) ≤ 18.5 cm	RMSEz (Bathymetric) ≤ 18.5 cm	RMSEz (Bathymetric) ≤ 18.5 cm	RMSEz (Bathymetric) ≤ 18.5 cm
	95% Confidence Level (Bathymetric) ≤ 36.3 cm	95% Confidence Level (Bathymetric) ≤ 36.3 cm	95% Confidence Level (Bathymetric) ≤ 36.3 cm	95% Confidence Level (Bathymetric) ≤ 36.3 cm

All areas were surveyed with an opposing flight line side-lap of $\geq 60\%$ ($\geq 100\%$ overlap) in order to reduce laser shadowing and increase surface laser painting. To accurately solve for laser point position (geographic coordinates x, y and z), the positional coordinates of the airborne sensor and the attitude of the aircraft were recorded continuously throughout the lidar data collection mission. Position of the aircraft was measured twice per second (2 Hz) by an onboard differential GPS unit, and aircraft attitude was measured 200 times per second (200 Hz) as pitch, roll and yaw (heading) from an onboard inertial measurement unit (IMU). To allow for post-processing correction and calibration, aircraft and sensor position and attitude data are indexed by GPS time.

Table 6: Flight Missions by Date

Date	Flight #	Start Time (Adjusted GPS)	End Time (Adjusted GPS)
07/26/2021	1	311331684	311346183
07/27/2021	1	311416223	311423292
07/27/2021	2	311425898	311432502
07/28/2021	1	311502606	311516933

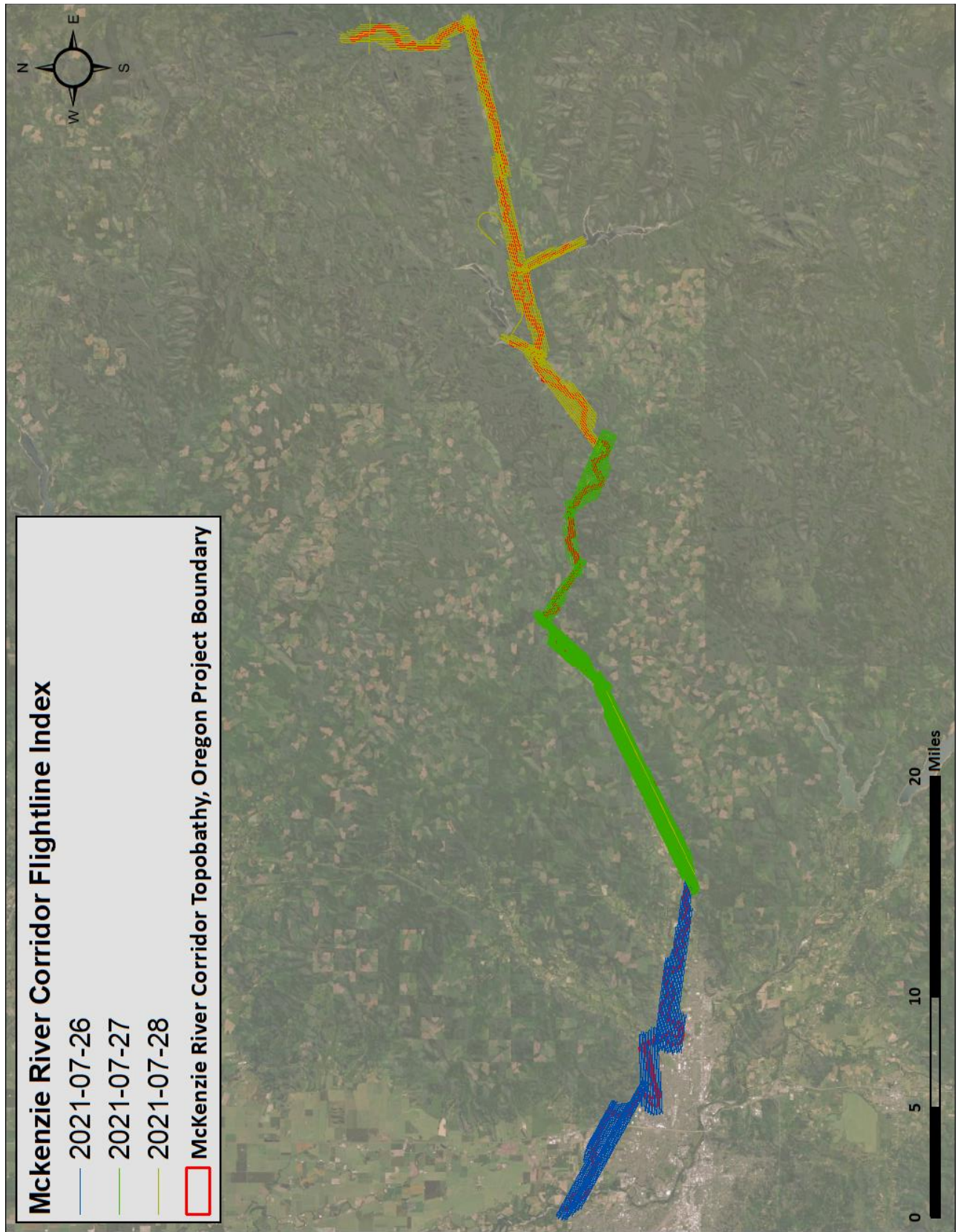


Figure 6: McKenzie River corridor Flightline Map

Digital Imagery

Aerial imagery was co-acquired (with the lidar) using a PhaseOne iXM-RS100F digital camera (Table 7). The PhaseOne is a medium format aerial mapping camera which collects imagery in three spectral bands (Red, Green, Blue). While acquisition windows targeted peak solar angles to reduce shadowing and sun glint in the imagery, optimal conditions for imagery collection may not have always been met as flight planning prioritized bathymetric lidar collection.

Table 7: Camera manufacturer's specifications

PhaseOne iXM-RS100F	
Focal Length	70 mm
Spectral Bands	Red, Green, Blue
Pixel Size	4.6 μm
Image Size	11,608 x 8,708 pixels
Frame Rate	GPS triggered
FOV	42° x 32°
Date Format	8bit TIFF

For the McKenzie River Corridor site, 8,934 images were collected with 60% along track overlap and 30% sidelap between frames. The acquisition flight parameters were designed to yield a native pixel resolution of ≤ 0.5 ft. Orthophoto specifications particular to the McKenzie River Corridor project are in Table 8.

Table 8: Project-specific orthophoto specifications

Digital Orthophotography Specifications	
Ground Sampling Distance (GSD)	≤ 0.5 ft pixel size
Along Track Overlap	$\geq 60\%$
Cross Track Overlap	$\geq 30\%$
Height Above Ground Level (AGL)	400 m
GPS PDOP	≤ 3.0
GPS Satellite Constellation	≥ 6

Ground Survey

Ground control surveys, including monumentation, and ground survey points (GSPs), were conducted to support the airborne acquisition. Ground control data were used to geospatially correct the aircraft positional coordinate data and to perform quality assurance checks on final lidar data.



Figure 8: Existing NGS Monument QE2666



Figure 7: NV5-Established monument MCKZ_BATHY_01

Base Stations

Base Stations were used for collection of ground survey points using real time kinematic (RTK), post-processed kinematic (PPK), fast static (FS), and total station (TS) survey techniques.

Base station locations were selected with consideration for satellite visibility, field crew safety, and optimal location for GSP coverage. NV5 Geospatial utilized two permanent real-time network (RTN) base stations from the Oregon Real-time GNSS Network (ORGN). NV5 Geospatial also established seven new monuments, and utilized two existing monuments, including one existing NV5 monument set using 5/8" x 30" rebar topped with stamped 2 1/2" aluminum caps, and one NGS monument (Table 9, Figure 7, and Figure 8). New monumentation was set using 6" mag hub nails with orange survey washers. NV5's professional land surveyor, Evon Silvia (ORPLS#81104) oversaw and certified the ground survey.

Table 9: Monument positions for the McKenzie River Corridor acquisition.
Coordinates are on the NAD83 (2011) datum, epoch 2010.00

Monument ID	Owner	Latitude	Longitude	Ellipsoid (meters)
LANE_75	NV5 AL Cap	44° 09' 14.03715"	-122° 21' 22.49441"	302.426
MCKZ_BATHY_01	NV5 Nail	44° 04' 00.65902"	-122° 48' 57.30284"	159.484
MCKZ_BATHY_03	NV5 Nail	44° 04' 10.93050"	-122° 53' 32.07305"	158.767
MCKZ_BATHY_04	NV5 Nail	44° 05' 56.64561"	-122° 41' 53.61384"	184.12
MCKZ_BATHY_05	NV5 Nail	44° 09' 09.42889"	-122° 14' 11.94364"	498.725
MCKZ_USGS_01	NV5 Nail	44° 05' 03.45164"	-122° 19' 35.36173"	418.288
MCKZ_USGS_02	NV5 Nail	44° 10' 04.39763"	-122° 09' 32.76221"	400.634
MCKZ_USGS_10	NV5 Nail	44° 16' 36.39646"	-122° 08' 09.55405"	1336.935
LPSB	ORGN	44° 03' 04.40923"	-123° 05' 24.24852"	118.092
OB3C	ORGN	44° 03' 57.45920"	-123° 05' 53.27962"	112.197
QE2666	NGS	44° 08' 44.29942"	-122° 34' 13.99785"	221.1

NV5 utilized static Global Navigation Satellite System (GNSS) data collected at 1 Hz recording frequency for each base station. During post-processing, the static GNSS data was triangulated with nearby

Continuously Operating Reference Stations (CORS) using the Online Positioning User Service (OPUS¹) for precise positioning. Multiple independent sessions over the same monument were processed to confirm antenna height measurements and to refine position accuracy.

Monuments were established according to the national standard for geodetic control networks, as specified in the Federal Geographic Data Committee (FGDC) Geospatial Positioning Accuracy Standards for geodetic networks.² This standard provides guidelines for classification of monument quality at the 95% confidence interval as a basis for comparing the quality of one control network to another. The monument rating for this project is shown in Table 10.

Table 10: Federal Geographic Data Committee monument rating for network accuracy

Direction	Rating
1.96 * St Dev _{NE} :	0.050 m
1.96 * St Dev _z :	0.050 m

For the McKenzie River Corridor Lidar project, the monument coordinates contributed no more than 5.6 cm of positional error to the geolocation of the final ground survey points and lidar, with 95% confidence.

Ground Survey Points (GSPs)

Ground survey points were collected using real time kinematic (RTK), post-processed kinematic (PPK), and fast-static (FS) survey techniques. For RTK surveys, a roving receiver receives corrections from a nearby base station or Real-Time Network (RTN) via radio or cellular network, enabling rapid collection of points with relative errors less than 1.5 cm horizontal and 2.0 cm vertical. PPK and FS surveys compute these corrections during post-processing to achieve comparable accuracy. RTK and PPK surveys record data while stationary for at least five seconds, calculating the position using at least three one-second epochs. FS surveys record observations for up to fifteen minutes on each GSP in order to support longer baselines. All GSP measurements were made during periods with a Position Dilution of Precision (PDOP) of ≤ 3.0 with at least six satellites in view of the stationary and roving receivers. See Table 11 for NV5 ground survey equipment information.

GSPs were collected in areas where good satellite visibility was achieved on paved roads and other hard surfaces such as gravel or packed dirt roads. GSP measurements were not taken on highly reflective surfaces such as center line stripes or lane markings on roads due to the increased noise seen in the laser returns over these surfaces. GSPs were collected within as many flightlines as possible; however, the distribution of GSPs depended on ground access constraints and monument locations and may not be equitably distributed throughout the study area (Figure 9).

¹ OPUS is a free service provided by the National Geodetic Survey to process corrected monument positions.
<http://www.ngs.noaa.gov/OPUS/>.

² Federal Geographic Data Committee, Geospatial Positioning Accuracy Standards (FGDC-STD-007.2-1998). Part 2: Standards for Geodetic Networks, Table 2.1, page 2-3. <http://www.fgdc.gov/standards/projects/FGDC-standards-projects/accuracy/part2/chapter2>






Table 11: NV5 Geospatial ground survey equipment identification

Receiver Model	Antenna	OPUS Antenna ID	Use
Trimble R6 Model 3	Integrated Antenna	TRM_R6-3	Static
Trimble R7	Zephyr GNSS Geodetic Model 2 RoHS	TRM57971.00	Static
Trimble R8 Model 2	Integrated Antenna	TRMR8_GNSS	Rover
Trimble R8 Model 3	Integrated Antenna	TRMR8_GNSS3	Static & Rover
Nikon NPL-322+ 5" P Total Station		n/a	VVA
Trimble M3 Total Station		n/a	VVA

Land Cover Class

In addition to ground survey points, land cover class check points were collected throughout the study area to evaluate vertical accuracy. Non-vegetated or vegetated check points were collected using a Nikon and Trimble Total Stations. Vertical accuracy statistics were calculated for all land cover types to assess confidence in the lidar derived ground models across land cover classes (Table 12, see Lidar Accuracy Assessments, page 30).

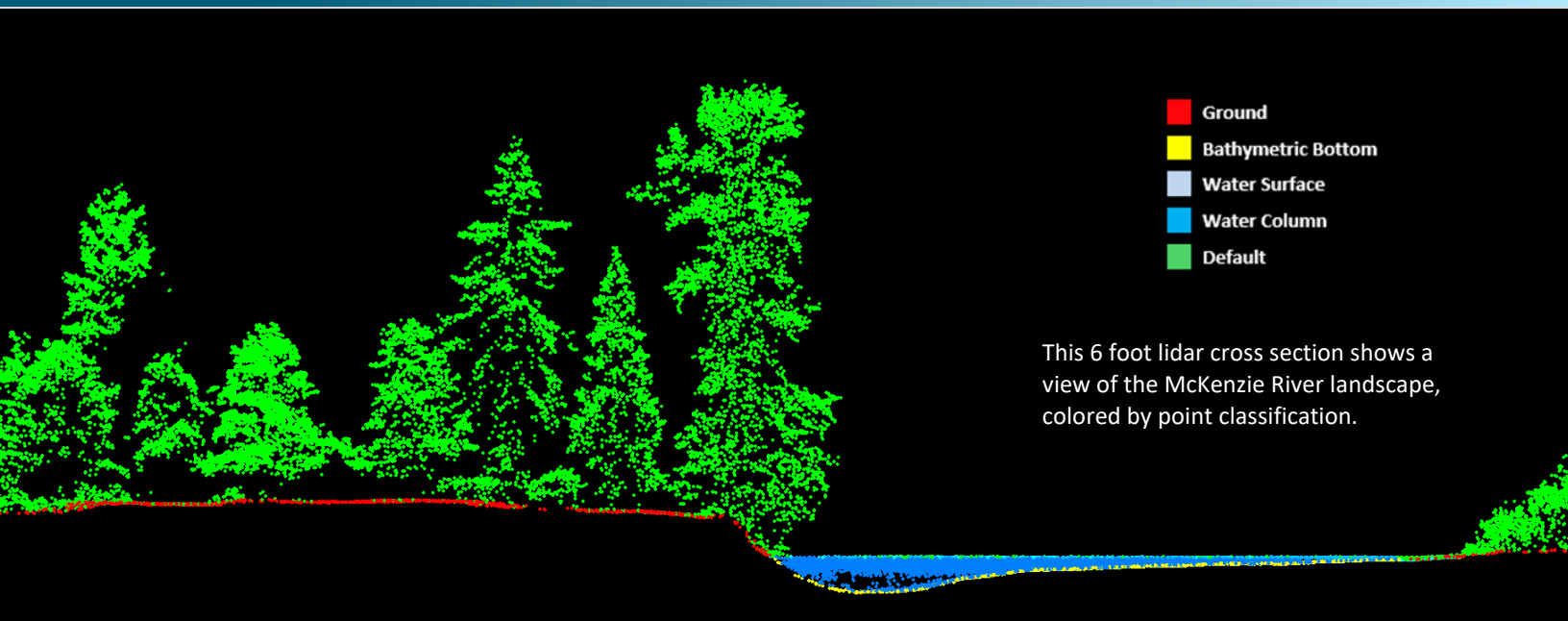
Table 12: Land Cover Types and Descriptions

Land Cover Type	Land Cover Code	Example	Description	Accuracy Assessment Type
Shrub	SHRUB		Low growth shrub	VVA
Tall Grass	TALL_GRASS		Herbaceous grasslands in advanced stages of growth	VVA
Deciduous Forest	DEC_FOR CON_FOR MX_FOR		Forested areas dominated by deciduous and/or coniferous species	VVA
Bare Earth	GVL LARGE_GVL DIRT SMALL_COBBL COBBLE		Areas of bare earth surface such as dirt, and gravel and cobble of varying sizes	NVA
Urban	URBAN PVD		Areas dominated by urban development, including parks	NVA

USGS Survey Collaboration

Along with NV5's field efforts, USGS personnel conducted additional field observations during topobathymetric lidar collection. NV5 and USGS collaborated to create a field work plan allowing USGS scientists to place field equipment along and within the channel for later analysis. NV5 examined lidar data for detection of some of these field equipment within the lidar data but made no conclusions. Within the provided images in Appendix B of one of the target sites displaying the lidar point cloud colorized by point classification, yellow represents potential targets and pink is used to represent high intensity backscatter surrounding the target. The field plan and images of NV5's examination can be found in Appendix B.

PROCESSING



Topobathymetric Lidar Data

Upon completion of data acquisition, NV5 processing staff initiated a suite of automated and manual techniques to process the data into the requested deliverables. Processing tasks included GPS control computations, smoothed best estimate trajectory (SBET) calculations, kinematic corrections, calculation of laser point position, sensor and data calibration for optimal relative and absolute accuracy, and lidar point classification (Table 13).

Riegl's RiProcess software was used to facilitate bathymetric return processing. Once bathymetric points were differentiated, they were spatially corrected for refraction through the water column based on the angle of incidence of the laser. NV5 refracted water column points using NV5's proprietary LAS processing software, Las Monkey. The resulting point cloud data was classified using both manual and automated techniques. Processing methodologies were tailored for the landscape. Brief descriptions of these tasks are shown in Table 14.

Table 13: ASPRS LAS classification standards applied to the McKenzie River Corridor dataset

Classification Number	Classification Name	Classification Description
1	Default/Unclassified	Laser returns that are not included in the ground class, composed of vegetation and anthropogenic features
1-W	Edge Clip/Withheld	Laser returns at the outer edges of flightlines that are geometrically unreliable
2	Ground	Laser returns that are determined to be ground using automated and manual cleaning algorithms
7-W	Low Noise/Withheld	Laser returns that are often associated with birds, scattering from reflective surfaces, or artificial points below the ground surface
9	Water	NIR laser returns that are determined to be water using automated and manual cleaning algorithms
17	Bridge	Bridge decks
18-W	High Noise/Withheld	Laser returns that are often associated with birds or scattering from reflective surfaces
40	Bathymetric Bottom	Refracted Riegl sensor returns that fall within the water's edge breakline which characterize the submerged topography
41	Water Surface	Green laser returns that are determined to be water surface points using automated and manual cleaning algorithms
45	Water Column	Refracted Riegl sensor returns that are determined to be water using automated and manual cleaning algorithms

Table 14 Lidar processing workflow

Lidar Processing Step	Software Used
Resolve kinematic corrections for aircraft position data using kinematic aircraft GPS and static ground GPS data. Develop a smoothed best estimate of trajectory (SBET) file that blends post-processed aircraft position with sensor head position and attitude recorded throughout the survey.	POSPac MMS v.8.5
Calculate laser point position by associating SBET position to each laser point return time, scan angle, intensity, etc. Create raw laser point cloud data for the entire survey in *.las (ASPRS v. 1.4) format. Convert data to orthometric elevations by applying a geoid correction.	RiProcess v1.8.5 Lidar Launcher 1.1 (NV5 proprietary software) Las Monkey 2.6 (NV5 proprietary software)
Import raw laser points into manageable blocks to perform manual relative accuracy calibration and filter erroneous points. Classify ground points for individual flight lines.	TerraScan v.19
Using ground classified points per each flight line, test the relative accuracy. Perform automated line-to-line calibrations for system attitude parameters (pitch, roll, heading), mirror flex (scale) and GPS/IMU drift. Calculate calibrations on ground classified points from paired flight lines and apply results to all points in a flight line. Use every flight line for relative accuracy calibration.	TerraMatch v.19 RiProcess v1.8.5
Apply refraction correction to all subsurface returns.	Las Monkey 2.6 (NV5 proprietary software)
Classify resulting data to ground and other client designated ASPRS classifications (Table 13). Assess statistical absolute accuracy via direct comparisons of ground classified points to ground control survey data.	TerraScan v.19 TerraModeler v.19
Generate bare earth models as triangulated surfaces. Generate highest hit models as a surface expression of all classified points. Export all surface models as Cloud Optimized GeoTIFFs (.tif) format at a 2.0 foot pixel resolution.	Las Product Creator 3.0 (NV5 proprietary software) ArcMap v. 10.3.1

Bathymetric Refraction

Green lidar pulses that enter the water column must have their position corrected for refraction of the light beam as it passes through the water and its resulting decreased speed. NV5 has developed proprietary software (Las Monkey) to perform this processing based on Snell's law. The first step is to develop a water surface model (WSM) from the NIR lidar water surface returns. The water surface model used for refraction is generated using NIR points within the breaklines defining the water's edge. Points are filtered and edited to obtain the most accurate representation of the water surface and are used to create a water surface model TIN. A TIN model is preferable to a raster based water surface model to obtain the most accurate angle of incidence during refraction.

Once the WSM is generated, the Las Monkey refraction software then intersects the partially submerged green pulses with the WSM to determine the angle of incidence with the water surface and the submerged component of the pulse vector. This provides the information necessary to correct the position of underwater points by adjusting the submerged vector length and orientation. After refraction, the points are compared against bathymetric check points to assess accuracy.

Lidar Derived Products

Because hydrographic laser scanners penetrate the water surface to map submerged topography, this affects how the data should be processed and presented in derived products from the lidar point cloud. The following discusses certain derived products that vary from the traditional (NIR) specification and delivery format.

Topobathymetric DEMs

Bathymetric bottom returns can be limited by depth, water clarity, and bottom surface reflectivity. Water clarity and turbidity affects the depth penetration capability of the green wavelength laser with returning laser energy diminishing by scattering throughout the water column. Additionally, the bottom surface must be reflective enough to return remaining laser energy back to the sensor at a detectable level. Although the predicted depth penetration range of the Riegl VQ-880-GII sensor is 1.5 Secchi depths on brightly reflective surfaces, it is not unexpected to have no bathymetric bottom returns in turbid or non-reflective areas.

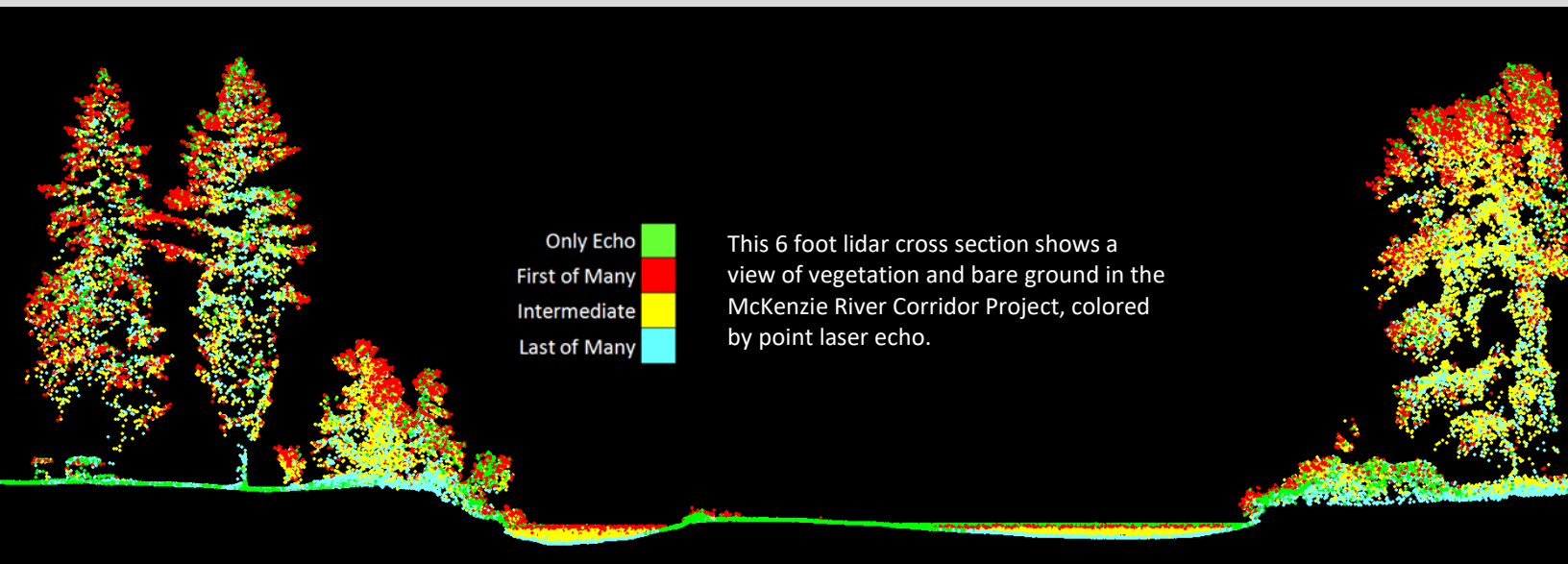
As a result, creating digital elevation models (DEMs) presents a challenge with respect to interpolation of areas with no returns. Traditional DEMs are "unclipped", meaning areas lacking ground returns are interpolated from neighboring ground returns (or breaklines in the case of hydro-flattening), with the assumption that the interpolation is close to reality. In bathymetric modeling, these assumptions are prone to error because a lack of bathymetric returns can indicate a change in elevation that the laser can no longer map due to increased depths. The resulting void areas may suggest greater depths, rather than similar elevations from neighboring bathymetric bottom returns. Therefore, NV5 created a water polygon with bathymetric coverage to delineate areas with successfully mapped bathymetry. This shapefile was used to control the extent of the delivered clipped topobathymetric model to avoid false triangulation (interpolation from TIN'ing) across areas in the water with no bathymetric returns.

Digital Imagery

As with the NIR lidar, the collected digital imagery went through multiple processing steps to create final orthophoto products. Initially, a boresight calibration flight was conducted to compute the rotational offset between the IMU and camera frame of reference. Boresight corrections allow for direct georefencing of imagery without aerial triangulation. Next, raw images were geometrically corrected to remove lens distortion using the camera factory calibration report. Camera position and orientation were then calculated as Exterior Orientations (EO) by linking the time of image capture to the smoothed best estimate of trajectory (SBET) file created during lidar post-processing. Orthophotos were output using the EO and lidar derived bare earth model and finally mosaicked using global color balancing and automatically generated seam lines. Due to the supplemental nature of the digital imagery, minimal manual seam editing or bridge rectification was performed; in some instances where bridges occupy multiple photos or are non nadir to the camera, slight warping is visible.. The processing workflow for orthophotos is summarized in Table 15.

Table 15: Orthophoto processing workflow

Orthophoto Processing Step	Software Used
Calculate camera misalignment angles from a system boresight flight conducted close to the project area	POSPac MMS v8.5
Resolve kinematic corrections for aircraft position data using IMU, kinematic aircraft GPS and Applanix PPRTX data. Develop a smoothed best estimate of trajectory (SBET) file that blends post-processed aircraft position with sensor head position and attitude recorded throughout the survey.	POSPac MMS v8.5
Calculate exterior orientation (EO) for each image event by linking the event time stamps with the SBET and boresight misalignment angles.	POSPac MMS v8.5
Convert raw imagery data into geometrically corrected TIFF images.	iX Capture v3.4
Import DEM and orthorectify image frames	Inpho OrthoMaster v10.02
Mosaic orthorectified imagery blending automated and manually drawn seams between photos and applying global color balancing to the project.	Inpho OrthoVista/Seameditor v10.0.2



Bathymetric Lidar

An underlying principle for collecting hydrographic lidar data is to survey near-shore areas that can be difficult to collect with other methods, such as multi-beam sonar, particularly over large areas. In order to determine the capability and effectiveness of the bathymetric lidar, several parameters were considered; depth penetrations below the water surface, bathymetric return density, and spatial accuracy.

Mapped Bathymetry and Depth Penetration

The specified depth penetration range of the Riegl VQ-880-GII sensor is 1.5 secchi depth; therefore, bathymetry data below one secchi depth at the time of acquisition is not to be expected. To assist in evaluating performance results of the sensor, a polygon layer was created to delineate areas where bathymetry was successfully mapped.

This shapefile was used to control the extent of the delivered clipped topo-bathymetric model and to avoid false triangulation across areas in the water with no returns. Insufficiently mapped areas were identified by triangulating bathymetric bottom points with an edge length maximum of 15.2 feet. This ensured all areas of no returns ($> 97 \text{ ft}^2$), were identified as data voids. Overall NV5 Geospatial successfully mapped 97.59% of the identified bathymetric area for the McKenzie River Corridor project. Of the areas successfully mapped, 78.16% had a calculated depth of 0 – 4.0 ft, 17.82% had a calculated depth of 4.1 - 8.0 ft, 3.30% had a calculated depth of 8.1 – 12.0 ft, and the remaining 0.72% had a calculated depth between 12.1 ft and 25.2 ft.

Lidar Point Density

First Return Point Density

The acquisition parameters were designed to acquire an average first-return density of 8 points/m². First return density describes the density of pulses emitted from the laser that return at least one echo to the system. Multiple returns from a single pulse were not considered in first return density analysis. Some types of surfaces (e.g., breaks in terrain, water and steep slopes) may have returned fewer pulses than originally emitted by the laser.

First returns typically reflect off the highest feature on the landscape within the footprint of the pulse. In forested or urban areas the highest feature could be a tree, building or power line, while in areas of unobstructed ground, the first return will be the only echo and represents the bare earth surface.

The average first-return density of the McKenzie River Corridor Lidar project was 3.24 points/ft² (34.85 points/m²) (Table 16). The statistical and spatial distributions of all first return densities per 100 m x 100 m cell are portrayed in Figure 10 and Figure 12.

Bathymetric and Ground Classified Point Densities

The density of ground classified lidar returns and bathymetric bottom returns were also analyzed for this project. Terrain character, land cover, and ground surface reflectivity all influenced the density of ground surface returns. In vegetated areas, fewer pulses may have penetrated the canopy, resulting in lower ground density. Similarly, the density of bathymetric bottom returns was influenced by turbidity, depth, and bottom surface reflectivity. In turbid areas, fewer pulses may have penetrated the water surface, resulting in lower bathymetric density.

The ground and bathymetric bottom classified density of lidar data for the McKenzie River Corridor project was 0.89 points/ft² (9.53 points/m²) (Table 16). The statistical and spatial distributions ground classified and bathymetric bottom return densities per 100 m x 100 m cell are portrayed in Figure 11 and Figure 13.

Additionally, for the McKenzie River Corridor project, density values of only bathymetric bottom returns were calculated for areas containing at least one bathymetric bottom return. Areas lacking bathymetric returns (voids) were not considered in calculating an average density value. Within the successfully mapped area, a bathymetric bottom return density of 1.09 points/ft² (11.75 points/m²) was achieved.

Table 16: Average Lidar point densities

Density Type	Point Density
First Returns	3.24 points/ft ² 34.85 points/m ²
Ground and Bathymetric Bottom Classified Returns	0.89 points/ft ² 9.53 points/m ²
Bathymetric Bottom Classified Returns	1.09 points/ft ² 11.75 points/m ²

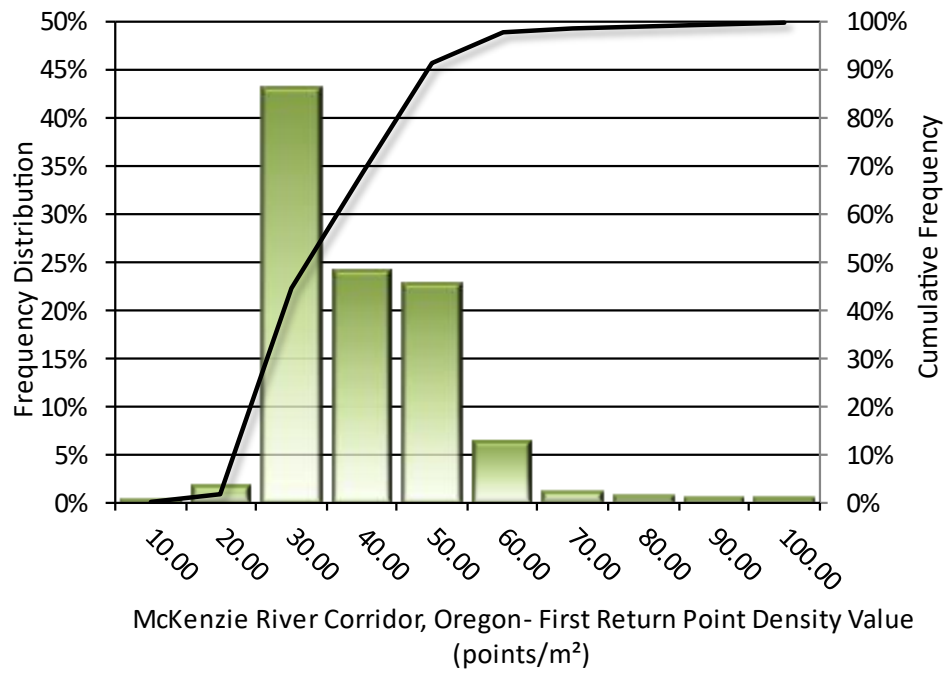


Figure 10: Frequency distribution of first return densities per 100 x 100 m cell

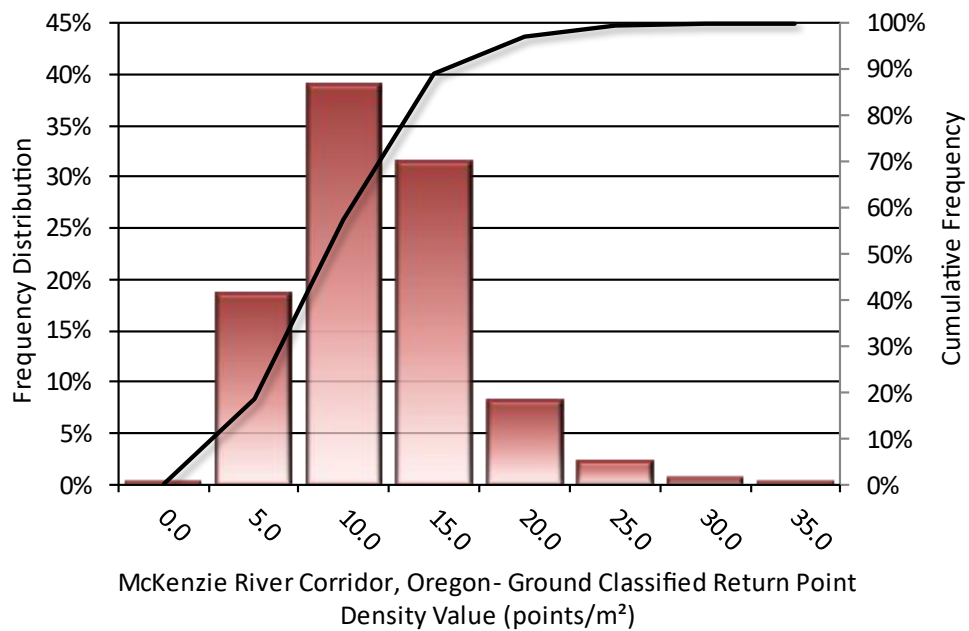


Figure 11: Frequency distribution of ground and bathymetric bottom classified return densities per 100 x 100 m cell

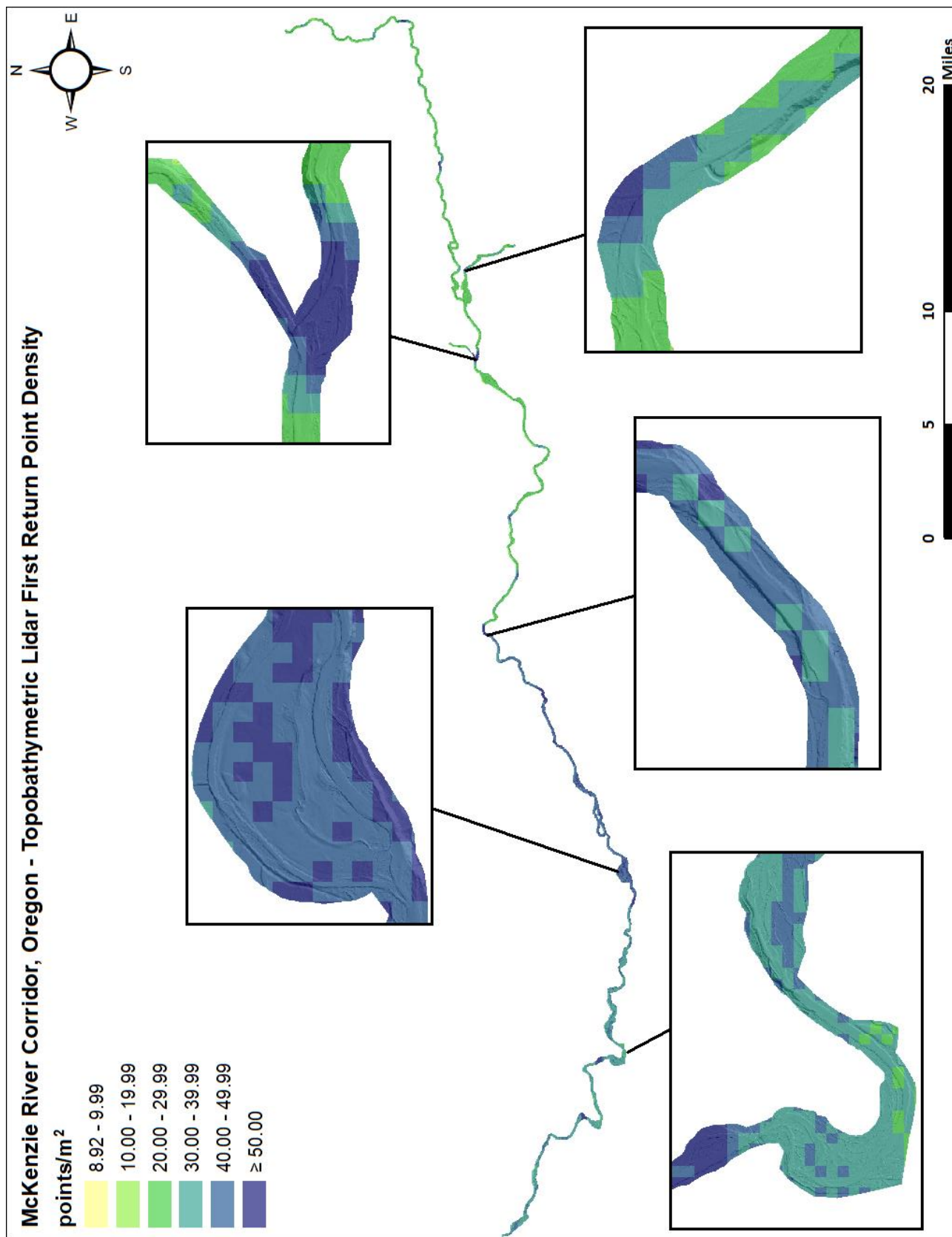


Figure 12: First return density map for the McKenzie River Corridor site (100 m x 100 m cells)

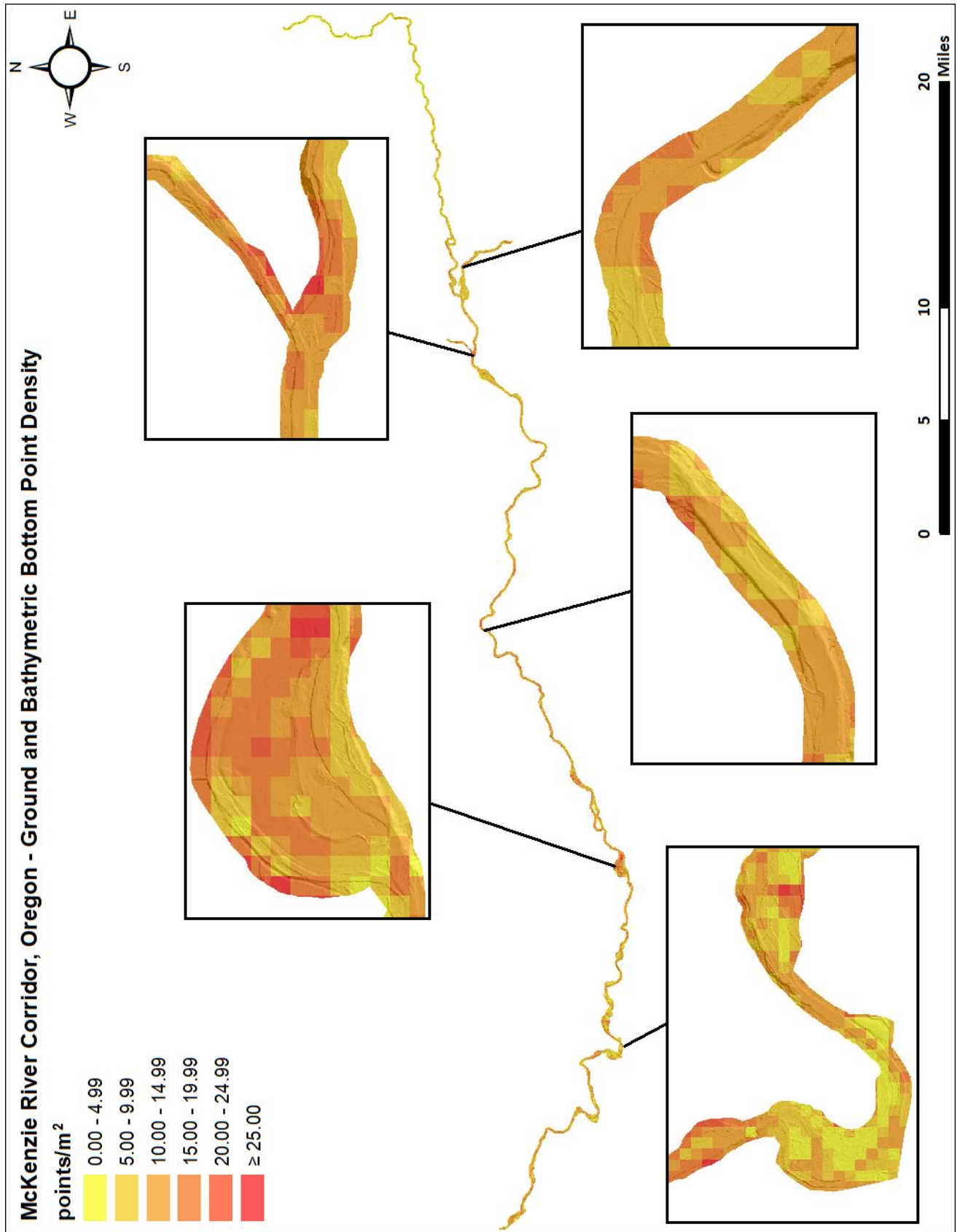


Figure 13: Ground and bathymetric bottom density map for the McKenzie River Corridor site (100 m x 100 m cells)

Lidar Accuracy Assessments

The accuracy of the lidar data collection can be described in terms of absolute accuracy (the consistency of the data with external data sources) and relative accuracy (the consistency of the dataset with itself). See Appendix A for further information on sources of error and operational measures used to improve relative accuracy.

Lidar Non-Vegetated Vertical Accuracy

Absolute accuracy was assessed using Non-vegetated Vertical Accuracy (NVA) reporting designed to meet guidelines presented in the FGDC National Standard for Spatial Data Accuracy³. NVA compares known ground check point data that were withheld from the calibration and post-processing of the lidar point cloud to the triangulated surface generated by the classified lidar point cloud as well as the derived gridded bare earth DEM. NVA is a measure of the accuracy of lidar point data in open areas where the lidar system has a high probability of measuring the ground surface and is evaluated at the 95% confidence interval ($1.96 * RMSE$), as shown in Table 17.

The mean and standard deviation (sigma σ) of divergence of the ground surface model from ground check point coordinates are also considered during accuracy assessment. These statistics assume the error for x, y and z is normally distributed, and therefore the skew and kurtosis of distributions are also considered when evaluating error statistics. For the McKenzie River Corridor survey, 23 ground check points were withheld from the calibration and post-processing of the lidar point cloud, with resulting non-vegetated vertical accuracy of 0.234 feet (0.071 meters) as compared to the classified LAS, and 0.201 feet (0.061 meters) against the bare earth DEM, with 95% confidence (Figure 14 and Figure 15). NV5 also assessed absolute accuracy using 14 ground control points. Although these points were used in the calibration and post-processing of the lidar point cloud, they still provide a good indication of the overall accuracy of the lidar dataset, and therefore have been provided in Table 17 and Figure 16.

³ Federal Geographic Data Committee, ASPRS POSITIONAL ACCURACY STANDARDS FOR DIGITAL GEOSPATIAL DATA EDITION 1, Version 1.0, NOVEMBER 2014.
https://www.asprs.org/a/society/committees/standards/Positional_Accuracy_Standards.pdf.

Table 17: Absolute accuracy results

Absolute Vertical Accuracy			
	NVA, as compared to Classified LAS	NVA, as compared to Bare Earth DEM	Ground Control Points
Sample	23 points	23 points	14 points
95% Confidence (1.96*RMSE)	0.234 ft	0.201 ft	0.188 ft
	0.071 m	0.061 m	0.057 m
Average	0.009 ft	0.019 ft	0.014 ft
	0.003 m	0.006 m	0.004 m
Median	0.039 ft	0.043 ft	0.028 ft
	0.012 m	0.013 m	0.008 m
RMSE	0.119 ft	0.102 ft	0.096 ft
	0.036 m	0.031 m	0.029 m
Standard Deviation (1σ)	0.122 ft	0.103 ft	0.099 ft
	0.037 m	0.031 m	0.030 m

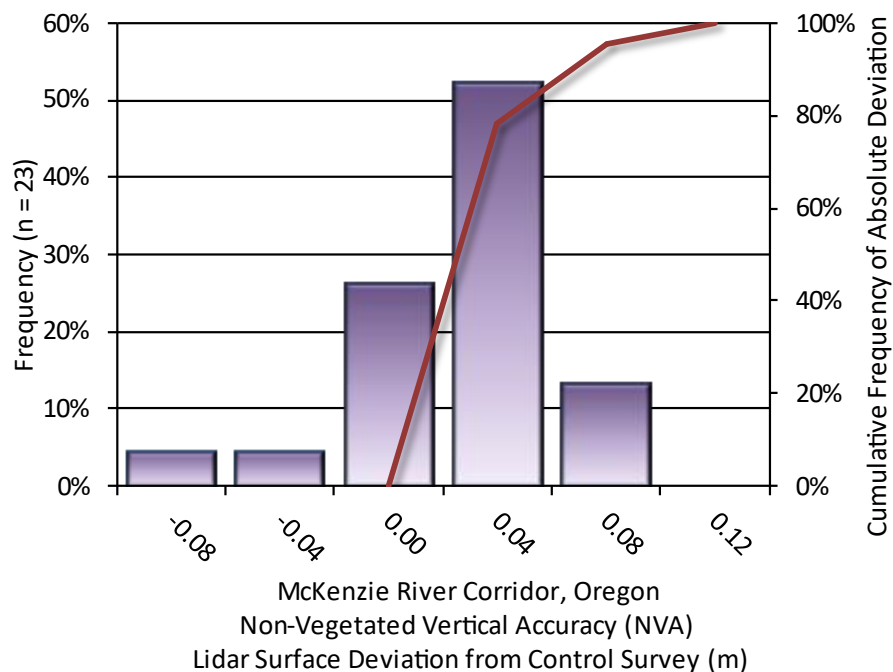


Figure 14: Frequency histogram for classified LAS deviation from ground check point values

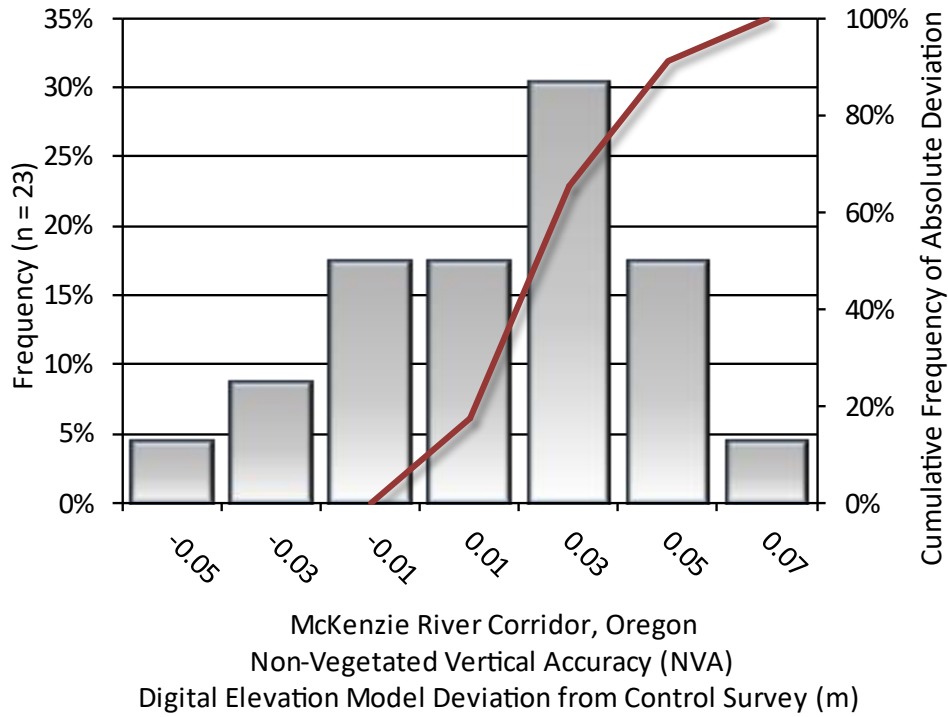


Figure 15: Frequency histogram for lidar bare earth DEM deviation from ground check point values

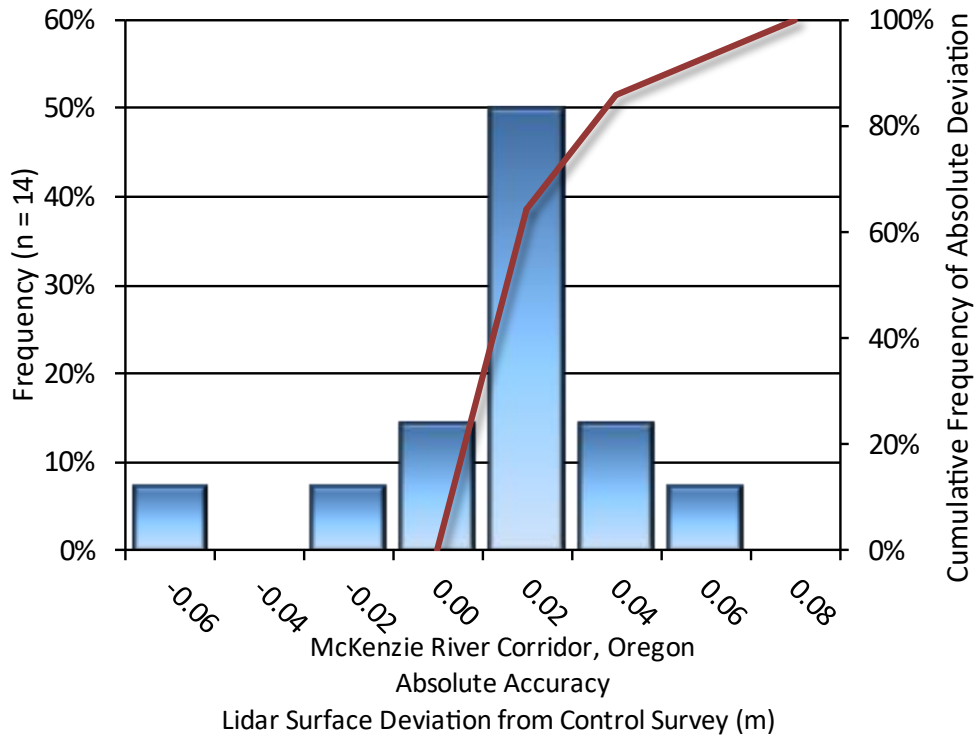


Figure 16: Frequency histogram for lidar surface deviation ground control point values

Lidar Bathymetric Vertical Accuracies

Bathymetric (submerged or along the water's edge) check points were also collected in order to assess the submerged surface vertical accuracy. Assessment of 174 submerged bathymetric check points resulted in a vertical accuracy of 0.454 (0.138 meters), while assessment of 49 wetted edge check points resulted in a vertical accuracy of 0.671 feet (0.205 meters), evaluated at 95% confidence interval (Table 19, Figure 19).

Table 18: Bathymetric Vertical Accuracy for the McKenzie River Corridor Project

Bathymetric Vertical Accuracy (VVA)		
	Submerged Bathymetric Check Points	Wetted Edge Bathymetric Check Points
Sample	174 points	49 points
95% Confidence (1.96*RMSE)	0.454 ft 0.138 m	0.671 ft 0.205 m
Average Dz	0.128 ft 0.039 m	0.007 ft 0.002 m
Median	0.123 ft 0.038 m	0.092 ft 0.028 m
RMSE	0.232 ft 0.071 m	0.343 ft 0.104 m
Standard Deviation (1σ)	0.193 ft 0.059 m	0.346 ft 0.105 m

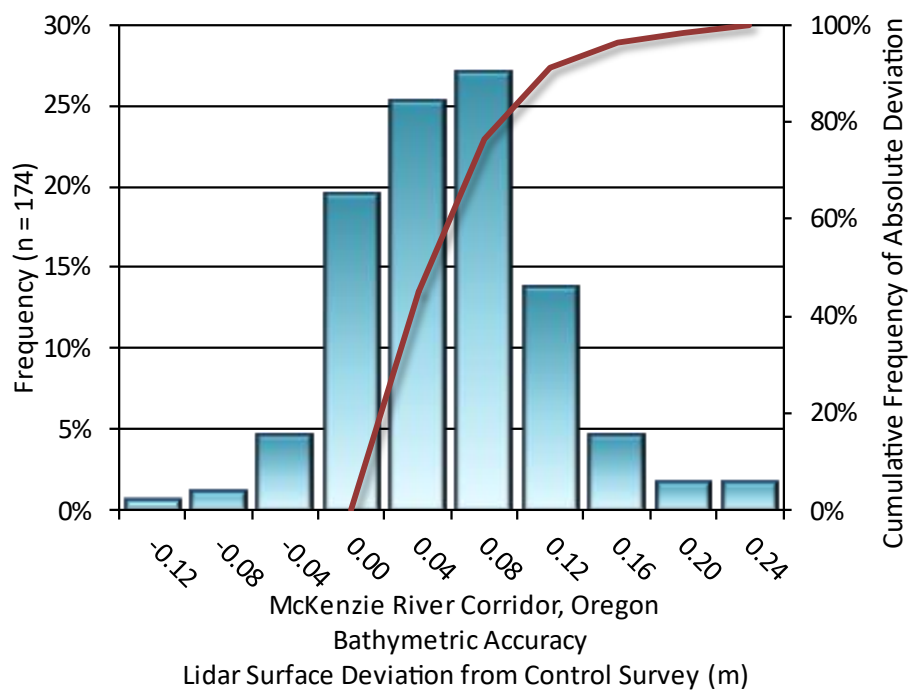


Figure 17: Frequency histogram for lidar surface deviation from submerged check point values

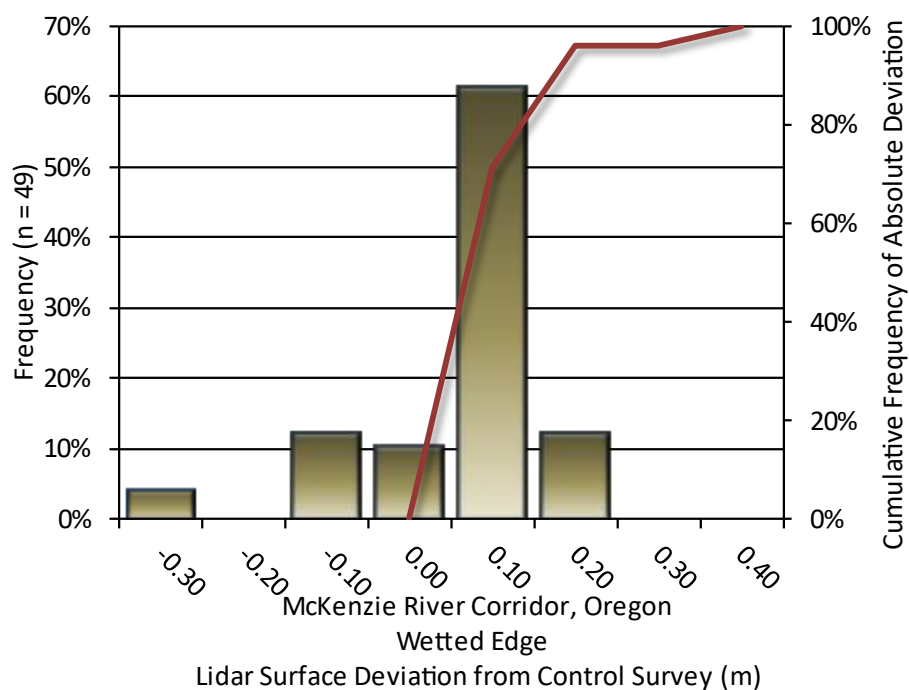


Figure 18: Frequency histogram for lidar surface deviation from wetted edge check point values

Lidar Vegetated Vertical Accuracies

NV5 also assessed vertical accuracy using Vegetated Vertical Accuracy (VVA) reporting. VVA compares known ground check point data collected over vegetated surfaces using land class descriptions to the triangulated ground surface generated by the ground classified lidar points. VVA is evaluated at the 95th percentile (Table 19, Figure 19).

Table 19: Vegetated Vertical Accuracy for the McKenzie River Corridor Project

Vegetated Vertical Accuracy (VVA)	
Sample	12 points
Average Dz	0.249 ft
	0.076 m
Median	0.208 ft
	0.064 m
RMSE	0.337 ft
	0.103 m
Standard Deviation (1 σ)	0.237 ft
	0.072 m
95 th Percentile	0.640 ft
	0.195 m

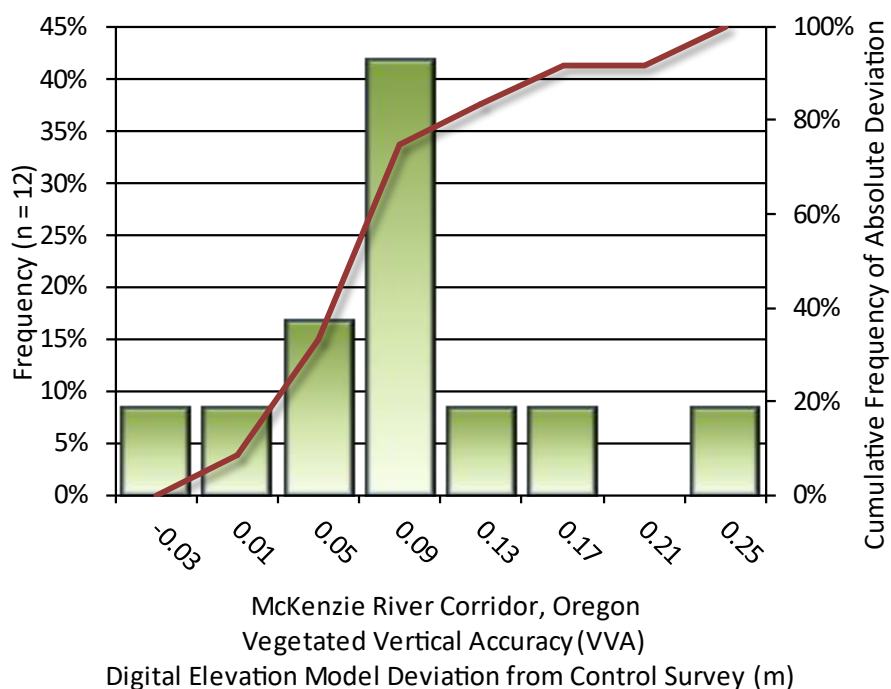


Figure 19: Frequency histogram for lidar surface deviation from all land cover class point values (VVA)

Lidar Relative Vertical Accuracy

Relative vertical accuracy refers to the internal consistency of the data set as a whole: the ability to place an object in the same location given multiple flight lines, GPS conditions, and aircraft attitudes. When the lidar system is well calibrated, the swath-to-swath vertical divergence is low (<0.10 meters). The relative vertical accuracy was computed by comparing the ground surface model of each individual flight line with its neighbors in overlapping regions. The average (mean) line to line relative vertical accuracy for the McKenzie River Corridor Lidar project was 0.054 feet (0.016 meters) (Table 20, Figure 20).

Table 20: Relative accuracy results

Relative Accuracy	
Sample	379 surfaces
Average	0.054 ft 0.016 m
Median	0.066 ft 0.020 m
RMSE	0.072 ft 0.022 m
Standard Deviation (1σ)	0.024 ft 0.007 m
1.96 σ	0.048 ft 0.015 m

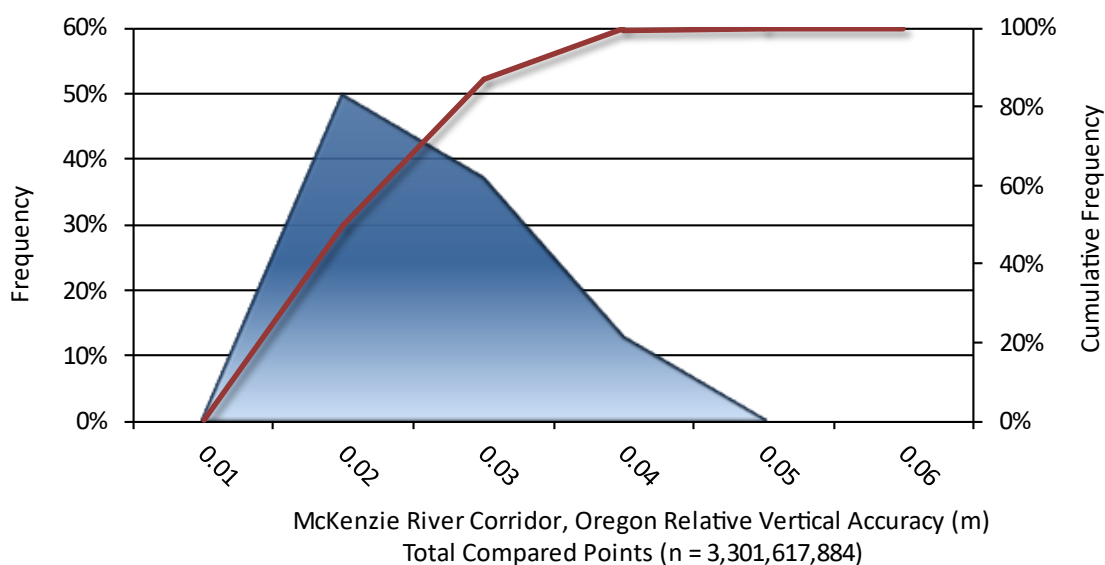


Figure 20: Frequency plot for relative vertical accuracy between flight lines

Lidar Horizontal Accuracy

Lidar horizontal accuracy is a function of Global Navigation Satellite System (GNSS) derived positional error, flying altitude, and INS derived attitude error. The obtained $RMSE_r$ value is multiplied by a conversion factor of 1.7308 to yield the horizontal component of the National Standards for Spatial Data Accuracy (NSSDA) reporting standard where a theoretical point will fall within the obtained radius 95 percent of the time.

All areas surveyed at a flying altitude of 400 meters, with an IMU error of 0.002 decimal degrees, and a GNSS positional error of 0.019 meters, were produced to meet 0.18 feet (0.05 m) horizontal accuracy at the 95% confidence level (Table 21).

All areas surveyed at a flying altitude of 600 meters, with an IMU error of 0.002 decimal degrees, and a GNSS positional error of 0.019 meters, were produced to meet 0.24 ft (0.07 m) horizontal accuracy at the 95% confidence level (Table 22).

Table 21: Horizontal Accuracy at 400 m flying altitude

Horizontal Accuracy	
RMSE _r	0.10 ft
	0.03 m
ACC _r	0.18 ft
	0.05 m

Table 22: Horizontal Accuracy at 600 m flying altitude

Horizontal Accuracy	
RMSE _r	0.14 ft
	0.04 m
ACC _r	0.24 ft
	0.07 m

Digital Imagery Accuracy Assessment

Due to the supplemental nature of the imagery collection, ground control was not surveyed for aerial triangulation, or accuracy assessment purposes of the final orthophoto products. Instead, initial exterior orientation parameters of the camera were adjusted using misalignment corrections from a camera boresight flight conducted prior to the McKenzie River Corridor photo project (see the Digital Imagery section for further details).

CERTIFICATIONS

NV5 Geospatial provided lidar services for the McKenzie River Corridor project as described in this report.

I, John English, have reviewed the attached report for completeness and hereby state that it is a complete and accurate report of this project.

John T. English

Jan 21, 2022

John English
Project Manager
NV5 Geospatial

I, Evon P. Silvia, PLS, being duly registered as a Professional Land Surveyor in and by the state of Oregon, hereby certify that the methodologies, static GNSS occupations used during airborne flights, and ground survey point collection were performed using commonly accepted Standard Practices. Field work conducted for this report was conducted between July 22 and August 3, 2021.

Accuracy statistics shown in the Accuracy Section of this Report have been reviewed by me and found to meet the "National Standard for Spatial Data Accuracy".

Evon P. Silvia

Jan 21, 2022

Evon P. Silvia, PLS
NV5 Geospatial
Corvallis, OR 97330

REGISTERED
PROFESSIONAL
LAND SURVEYOR

Evon P. Silvia

OREGON
JUNE 10, 2014
EVON P. SILVIA
81104LS

EXPIRES: 06/30/2022

GLOSSARY

1-sigma (σ) Absolute Deviation: Value for which the data are within one standard deviation (approximately 68th percentile) of a normally distributed data set.

1.96 * RMSE Absolute Deviation: Value for which the data are within two standard deviations (approximately 95th percentile) of a normally distributed data set, based on the FGDC standards for Non-vegetated Vertical Accuracy (FVA) reporting.

Accuracy: The statistical comparison between known (surveyed) points and laser points. Typically measured as the standard deviation (sigma σ) and root mean square error (RMSE).

Absolute Accuracy: The vertical accuracy of lidar data is described as the mean and standard deviation (sigma σ) of divergence of lidar point coordinates from ground survey point coordinates. To provide a sense of the model predictive power of the dataset, the root mean square error (RMSE) for vertical accuracy is also provided. These statistics assume the error distributions for x, y and z are normally distributed, and thus we also consider the skew and kurtosis of distributions when evaluating error statistics.

Relative Accuracy: Relative accuracy refers to the internal consistency of the data set; i.e., the ability to place a laser point in the same location over multiple flight lines, GPS conditions and aircraft attitudes. Affected by system attitude offsets, scale and GPS/IMU drift, internal consistency is measured as the divergence between points from different flight lines within an overlapping area. Divergence is most apparent when flight lines are opposing. When the lidar system is well calibrated, the line-to-line divergence is low (<10 cm).

Root Mean Square Error (RMSE): A statistic used to approximate the difference between real-world points and the lidar points. It is calculated by squaring all the values, then taking the average of the squares and taking the square root of the average.

Data Density: A common measure of lidar resolution, measured as points per square meter.

Digital Elevation Model (DEM): File or database made from surveyed points, containing elevation points over a contiguous area. Digital terrain models (DTM) and digital surface models (DSM) are types of DEMs. DTMs consist solely of the bare earth surface (ground points), while DSMs include information about all surfaces, including vegetation and man-made structures.

Intensity Values: The peak power ratio of the laser return to the emitted laser, calculated as a function of surface reflectivity.

Nadir: A single point or locus of points on the surface of the earth directly below a sensor as it progresses along its flight line.

Overlap: The area shared between flight lines, typically measured in percent. 100% overlap is essential to ensure complete coverage and reduce laser shadows.

Pulse Rate (PR): The rate at which laser pulses are emitted from the sensor; typically measured in thousands of pulses per second (kHz).

Pulse Returns: For every laser pulse emitted, the number of wave forms (i.e., echoes) reflected back to the sensor. Portions of the wave form that return first are the highest element in multi-tiered surfaces such as vegetation. Portions of the wave form that return last are the lowest element in multi-tiered surfaces.

Real-Time Kinematic (RTK) Survey: A type of surveying conducted with a GPS base station deployed over a known monument with a radio connection to a GPS rover. Both the base station and rover receive differential GPS data and the baseline correction is solved between the two. This type of ground survey is accurate to 1.5 cm or less.

Post-Processed Kinematic (PPK) Survey: GPS surveying is conducted with a GPS rover collecting concurrently with a GPS base station set up over a known monument. Differential corrections and precisions for the GNSS baselines are computed and applied after the fact during processing. This type of ground survey is accurate to 1.5 cm or less.

Scan Angle: The angle from nadir to the edge of the scan, measured in degrees. Laser point accuracy typically decreases as scan angles increase.

Native Lidar Density: The number of pulses emitted by the lidar system, commonly expressed as pulses per square meter.

APPENDIX A – ACCURACY CONTROLS

Relative Accuracy Calibration Methodology:

Manual System Calibration: Calibration procedures for each mission require solving geometric relationships that relate measured swath-to-swath deviations to misalignments of system attitude parameters. Corrected scale, pitch, roll and heading offsets were calculated and applied to resolve misalignments. The raw divergence between lines was computed after the manual calibration was completed and reported for each survey area.

Automated Attitude Calibration: All data was tested and calibrated using TerraMatch automated sampling routines. Ground points were classified for each individual flight line and used for line-to-line testing. System misalignment offsets (pitch, roll and heading) and scale were solved for each individual mission and applied to respective mission datasets. The data from each mission were then blended when imported together to form the entire area of interest.

Automated Z Calibration: Ground points per line were used to calculate the vertical divergence between lines caused by vertical GPS drift. Automated Z calibration was the final step employed for relative accuracy calibration.

Lidar accuracy error sources and solutions:

Type of Error	Source	Post Processing Solution
GPS (Static/Kinematic)	Long Base Lines	None
	Poor Satellite Constellation	None
	Poor Antenna Visibility	Reduce Visibility Mask
Relative Accuracy	Poor System Calibration	Recalibrate IMU and sensor offsets/settings
	Inaccurate System	None
Laser Noise	Poor Laser Timing	None
	Poor Laser Reception	None
	Poor Laser Power	None
	Irregular Laser Shape	None

Operational measures taken to improve relative accuracy:

Low Flight Altitude: Terrain following was employed to maintain a constant above ground level (AGL). Laser horizontal errors are a function of flight altitude above ground (about 1/3000th AGL flight altitude).

Focus Laser Power at narrow beam footprint: A laser return must be received by the system above a power threshold to accurately record a measurement. The strength of the laser return (i.e., intensity) is a function of laser emission power, laser footprint, flight altitude and the reflectivity of the target. While surface reflectivity cannot be controlled, laser power can be increased and low flight altitudes can be maintained.

Reduced Scan Angle: Edge-of-scan data can become inaccurate. The scan angle was reduced to a maximum of $\pm 20^\circ$ from nadir, creating a narrow swath width and greatly reducing laser shadows from trees and buildings.

Quality GPS: Flights took place during optimal GPS conditions (e.g., 6 or more satellites and PDOP [Position Dilution of Precision] less than 3.0). Before each flight, the PDOP was determined for the survey day. During all flight times, a dual frequency DGPS base station recording at 1 second epochs was utilized and a maximum baseline length between the aircraft and the control points was less than 13 nm at all times.

Ground Survey: Ground survey point accuracy (<1.5 cm RMSE) occurs during optimal PDOP ranges and targets a minimal baseline distance of 4 miles between GPS rover and base. Robust statistics are, in part, a function of sample size (n) and distribution. Ground survey points are distributed to the extent possible throughout multiple flight lines and across the survey area.

50% Side-Lap (100% Overlap): Overlapping areas are optimized for relative accuracy testing. Laser shadowing is minimized to help increase target acquisition from multiple scan angles. Ideally, with a 50% side-lap, the nadir portion of one flight line coincides with the swath edge portion of overlapping flight lines. A minimum of 50% side-lap with terrain-followed acquisition prevents data gaps.

Opposing Flight Lines: All overlapping flight lines have opposing directions. Pitch, roll and heading errors are amplified by a factor of two relative to the adjacent flight line(s), making misalignments easier to detect and resolve.

APPENDIX B – USGS SURVEY SUMMARY

Appendix B:

Accuracy Assessment and Validation Field Survey Plan and NV5 Observations of USGS Field Equipment: See separate document “Topobathymetric_Lidar_Report_OR_McKenzieRiverCorridor_Topobathy_2021-Appendix_B .pdf” for Appendix B.